International Conference on Innovative Research in Engineering, Management and Sciences
International Journal of Scientific Research in Computer Science, Engineering and Information Technology
© 2019 IJSRCSEIT | Volume 4 | Issue 9 | ISSN : 2456-3307

Characteristic Study of Combined effects of Dufour and Coriolis Force on Free Convection in a Rectangular Cavity with Isotropic and Anisotropic Porous Media

Sudhir Patel*[1], Dinesh P A[2], Suma S P[3]

*[1]Department of Mathematics, New Horizon College of Engineering Bangalore-560103, India
sudhirp@newhorizonindia.edu[1]
[2]Department of Mathematics Ramaiah Institute of Technology Bangalore-560054, India
dineshdpa@msrit.edu[2]
[3] Department of Mathematics Cambridge Institute of Technology Bangalore-560036, India
drsumasp@gmail.com[3]

ABSTRACT

This study investigates the effects of dufour and coriolis force on classic Rayleigh -Bènard problem for an laminar, viscous, unsteady incompressible fluid flow heated from below is extended to 3-dimesional convection in a finite geometry with isotropic and anisotropic porous media rotating with constant angular velocity. For the given physical set-up, g partial differential equations of the physical configuration are transformed to a set of non-dimensional ordinary differential equations using similarity transformation. This demands to apply Fourier series method to study the characteristic of velocity, temperature and concentration for the effect of Taylors number, Rayleigh number, Hartmann's number and Prandtl number for both anisotropic and isotropic porous media. The results of steam function and isotherms on various parameters have been discussed and found to be good agreement for the physical system.)

Keywords: Isotropic and anisotropic porous media, Free convection, Coriolis force, MHD.

I. INTRODUCTION

Among the different forms of energy, heat energy for its application in wide variety of fields has its own importance not only in industry but also in personal life. Humans are associated with the, utilization [1-3], generation [4], transformation [5] and convection [6] of heat energy management and conservation. In the last few decade research on thermally driven fluid flow and convection has considerably increased due to its applications diverse areas like, in meteorology, chemical food, metallurgical industries, nuclear reactor system, energy conservation and storage. Essential coupling between flow and thermal filed makes the buoyancy driven flows has not been investigated much. The problems in these flows are classified as free convection(external) and natural convection(internal) .

Gelfgat et al. [7] in 2001 studied of the effect of magnetic field on the an axisymmetric convective flow, convection in a vertical cylinder with a temperature variation on the sidewalls was considered. Galerkin method was applied to analysis the three dimensional stability of the flow.

Rayleigh–Be´nard convection exist when the horizontal wall is heated from below. This study has been done for various applications, particularly in

the field of electronics. Rayleigh–Be´nard convection is represented by non-linear partial differential equations for momentum, mass and energy whose resolution becomes ambiguous when the Rayleigh number exceeds a critical value. Many detailed investigations on Rayleigh–Be´nard convection, as well as reviews on this, like those of Yang [8] and Koschmieder [9].

The transformation from the conductive to the convective mode takes place at higher Rayleigh numbers than those for cavities with isothermal hot walls, and the flow in the central part of the cavity is more complex and non-permanent Fusegi et al. [10] and Janssen et al. [11].

Initially numerical studies of Natural convection flow were normally limited to two–dimensional configuration with comparatively low Rayleigh numbers (Ra). The fundamental ground of work was setup by de Vahl Davis et al [12] it gave original standard solutions for a square 2D cavity with 103 to 106 ; subsequently, Hortmann [13] came up with more accurate results by using the multi-grid method with a extremely finer mesh. Lot of others have duplicated the results with Ra up to 108 [14–17].

1.1 Nomenclature

a = width of the rectangular channel

β = Thermal expansion co-efficient

c = Specific hear at constant pressure

$\vec{g} = (0, 0, -g)$ acceleration due to gravity

h = Height of the rectangular channel

κ = Thermal diffusivity in isotropic case

$\kappa = (\kappa_x, \kappa_y, \kappa_z)$ Thermal diffusivity along x, y, z axis in anisotropic case

k = Permeability in isotropic case

$\vec{q} = (u, v, w)$ = Velocity of the fluid

R_a = Thermal Rayleigh Number

t = Time

T = Temperature

ΔT = Characteristic temperature difference

T_0 = Reference temperature

θ = Deviation from static temperature

ρ = Density

ρ_0 = Reference density

$(\rho c_v)_S, (\rho c_v)_f$ = Heat capacity per unit volume of the solid and fluid

x, y, z = Space coordinate

ν = Thermal viscosity

$\psi = \psi(x, y)$ = Streamline function

R_C = Solutal Rayleigh Number

S_0 = Reference Concentration

ΔS = Characteristic Concentration difference

S = Deviation from the static concentration

σ = Growth rate

$T_a = \frac{2\Omega d^2}{\nu}$ = Taylors Number

$\xi = \frac{k_x}{k_z}\left(\frac{h}{a}\right)^2$ = Anisotropic ratio

$\eta = \frac{\kappa_x}{\kappa_z}\left(\frac{h}{a}\right)^2$ = Aspect ratio

$\Omega = (0, 0, \Omega)$ = Uniform angular velocity of the system

$k = (k_x, k_y, k_z)$ Permeability along x,y,z axis in anisotropic case

S = Concentration

p_1 = Pressure

$p = p_1 - \frac{1}{2}|\Omega \times r|$

$\nabla = \left(\frac{\partial}{\partial x}, \frac{\partial}{\partial y}, \frac{\partial}{\partial z}\right)$ = Three dimensional gradient operator

$\nabla^2 = \left(\frac{\partial^2}{\partial x^2}, \frac{\partial^2}{\partial y^2}, \frac{\partial^2}{\partial z^2}\right)$ = Three dimensional Laplacian operator

Multiple attempts have been made on three-dimensional (3D) simulations, as the actual flow is always a 3D. the effects of a certain aspect of a ratio on flow patterns with Ra of order 106 was studied by Mallinson et al. [18]. Hysteretic behavior , observed by Labrosses et al. [19] using a pseudo-spectral solver. Trias et al. [20,21] investigated the 3D cavity of aspect ratio 4 with periodic lateral walls and showed that there is significant difference in the flow dynamics between two- dimension and three-dimension results. It is emphasized that natural convection flow in a three dimensional cubical cavity with adiabatic lateral walls has been comparatively explored less [22-24].

There is no work carried out by to understand the effect of concentration on the temperature. This effect can be understood with the dufour term which is introduced in the temperature equation. Here the main objective of the study is to understand the effect of dufour and coriolis force on classic Rayleigh -Bènard problem for an laminar, viscous, unsteady incompressible fluid flow heated from below is extended to 3-dimesional convection in a finite geometry with isotropic and anisotropic porous media rotating with constant angular velocity.

II. MATHEMATICAL FORMULATION

A 3-D free convection in a rectangular porous box, non-uniformly heated from down is considered. The porous media is considered to be saturated and an-isotropic by a incompressible homogeneous fluid. The rectangular box is of width a and height h, we choose vertical direction of the box as z axis, the

horizontal walls of the box are at z=(0,h) and the horizontal direction along the length of the box as x axis, vertical walls are at x = ± a/2, Fig. (1). In order to neglect the inertia terms and appeal to Boussinesq approximation Prandtl-Darcy number is assumed to be very large. The 3-D model of the Darcy-Boussinesq equations takes the formKeep your text and graphic files separate until after the text has been formatted and styled. Do not use hard tabs, and limit use of hard returns to only one return at the end of a paragraph. Do not add any kind of pagination anywhere in the paper. Do not number text heads-the template will do that for you.

$$\frac{\partial u}{\partial x}+\frac{\partial u}{\partial z}=0 \quad , \tag{2.1}$$

$$\frac{1}{\rho_0}\frac{\partial p}{\partial x}+\frac{\nu}{k_x}u-2\Omega v=0\,, \tag{2.2}$$

$$\frac{1}{\rho_0}\frac{\partial p}{\partial y}+\frac{\upsilon}{k_y}v+2\Omega u=0\,, \tag{2.3}$$

$$\frac{1}{\rho_0}\frac{\partial p}{\partial z}-\frac{\rho}{\rho_0}g+\frac{\upsilon}{k_z}w=0 \quad , \tag{2.4}$$

$$c\frac{\partial T}{\partial t}+v.\nabla T=\kappa_x\left(\frac{\partial^2 T}{\partial x^2}+\frac{\sigma_X}{c_S}\frac{\partial^2 S}{\partial x^2}\right)+\kappa_z\left(\frac{\partial^2 T}{\partial z^2}+\frac{\sigma_Z}{c_S}\frac{\partial^2 S}{\partial z^2}\right) \tag{2.5}$$

$$\frac{\partial S}{\partial t}+u\frac{\partial S}{\partial x}+w\frac{\partial S}{\partial z}=\sigma_x\frac{\partial^2 S}{\partial x^2}+\sigma_z\frac{\partial^2 S}{\partial z^2} \quad , \tag{2.6}$$

$$\rho=\rho_0\,[1-\beta(T-T_0)+\alpha(S-S_0\,)]\,. \tag{2.7}$$

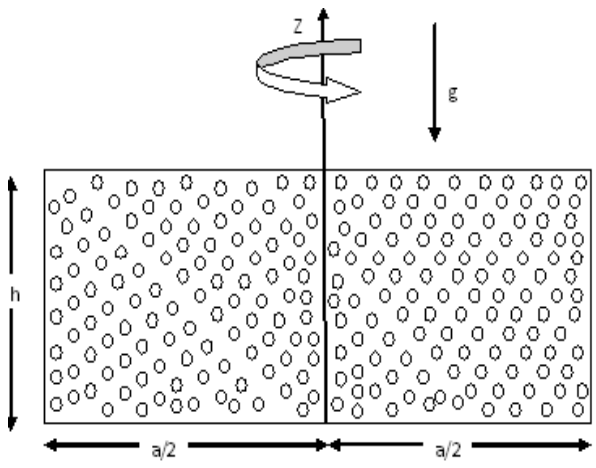

Fig. 1. Physical Configuration.

The lower and the upper walls of the box are at isothermal temperatures T0 andT0+ΔT here ΔT is the absolute temperature. All the walls of the box are considered to heat conducting and impermeable. From the equations (2.1) to (2.7) we get that a static conduction occurs if the constant temperature circulation depends linearly on z and is sovereign of x.

$$T=\left[T_0+\Delta T\left(1-\frac{z}{h}\right)\right]+\theta\,,$$

$$S=\left[S_0+\Delta S\left(1-\frac{z}{h}\right)\right]+s \tag{2.8}$$

Where θ and s are the deviations from the static temperature and concentration respectively.

Because the flow is axis symmetric, we represent the stream function $\psi=\psi(x,y)$ by

$$u=\frac{\partial\psi}{\partial z}, \qquad w=-\frac{\partial\psi}{\partial x}\,. \tag{2.9}$$

Non-dimensional terms are represented by asterisks

$$u=\frac{\kappa_x a u^*}{h^2}, v=\frac{\kappa_y a v^*}{h^2}, w=\frac{\kappa_z w^*}{h}, t=\frac{ch^2 t^*}{\kappa_z};$$

$$x=ax^*, y=ay^*, z=hz^*,$$

$$\psi=\frac{\kappa_z a\psi^*}{h},\ \theta=\Delta T\theta^*,\ T_0=\Delta T T_0^*,\ p=\frac{\nu k_z\rho_0 p^*}{k_z},\ S=\Delta S S^* \tag{2.10}$$

On introduction of above expressions into equations (2.1)-(2.7), the governing equation takes the form:

$$\left(\xi\frac{\partial^2}{\partial x^2}+\frac{\partial^2}{\partial z^2}\right)\psi+\xi R_a\frac{\partial\theta}{\partial x}-\xi R_S\frac{\partial s}{\partial x}-T_a\frac{\partial v}{\partial z}=0 \tag{2.11}$$

$$\chi\frac{\partial v}{\partial z}+T_a\frac{\partial^2\psi}{\partial z^2}=0 \quad , \tag{2.12}$$

$$P_c\left(\zeta\frac{\partial^2}{\partial x^2}+\frac{\partial^2}{\partial z^2}\right)S-\frac{\partial\psi}{\partial t}=\frac{\partial S}{\partial t}\,,$$

(2.13)

$$\left(\eta\frac{\partial^2}{\partial x^2}+\frac{\partial^2}{\partial z^2}\right)\theta+p_m\left(\zeta_1\frac{\partial^2}{\partial x^2}+\frac{\partial^2}{\partial z^2}\right)S-\frac{\partial\psi}{\partial x}=\frac{\partial\theta}{\partial t}\,.$$

(2.14)

Where, Rs is the Solutal Rayleigh number (or Darcy- Solutal Rayleigh number) and Ra is the Rayleigh number (or Darcy- Rayleigh number,is given by

$$R_S = \frac{\alpha g \Delta S k_z h}{\kappa_z \upsilon},\ p_m = \frac{\Delta S}{\Delta T}\left(\frac{\sigma_z}{C_S}\right),\ R_a = \frac{\beta g \Delta T k_z h}{\kappa_z \upsilon}. \tag{2.15}$$

The anisotropy aspect ratio of permeability and diffusivity of temperature are represented by ξ, η, ζ and χ

$$\xi = \frac{k_x}{k_z}\left(\frac{h}{a}\right)^2, \eta = \frac{\sigma_x}{\sigma_z}\frac{\kappa_x}{\kappa_z}\left(\frac{h}{a}\right)^2, \zeta = \frac{\sigma_x}{\sigma_z}\left(\frac{h}{a}\right)^2,$$

$$\zeta_1 = \frac{k_x}{k_z}\frac{\sigma_x}{\sigma_z}\left(\frac{h}{a}\right)^2,\ \chi = \frac{k_x}{k_z}\left(\frac{a}{h}\right)^2. \tag{2.16}$$

The boundary condition for absolutely impermeable boundaries and heat conducting walls is given by

$$S = \psi = \theta = \frac{\partial v}{\partial z} = 0 \text{ on } \begin{cases} x = -\frac{1}{2}, x = \frac{1}{2} & 0 < z < 1 \\ z = 0,\ z = 1 & -\frac{1}{2} < x < \frac{1}{2} \end{cases}. \tag{2.17}$$

III. STEADY FLOW PATTERNS AND LINEAR STABILITY

Free convection, mentioned by linear versions of the equation (2.11) to (2.14). The solution of these equations can be expended in Fourier series as

$$\psi = e^{\sigma t}\left[\frac{C_0}{2} + \sum_{n=1}^{\infty} C_n(x)\cos n\pi z + D_n(x)\sin n\pi z\right], \tag{3.1}$$

$$\theta = e^{\sigma t}\left[\frac{F_0}{2} + \sum_{n=1}^{\infty} F_n(x)\cos n\pi z + G_n(x)\sin n\pi z\right], \tag{3.2}$$

$$v = e^{\sigma t}\left[\frac{A_0}{2} + \sum_{n=1}^{\infty} A_n(x)\cos n\pi z + B_n(x)\sin n\pi z\right], \tag{3.3}$$

$$S = e^{\sigma t}\left[\frac{S_0}{2} + \sum_{n=1}^{\infty} S_n(x)\cos n\pi z + H_n(x)\sin n\pi z\right]. \tag{3.4}$$

Where $C_n, D_n, F_n, G_n, A_n, B_n, S_n$ and H_n are in terms of x only and the growth rate is represented σ. To satisfy the boundary conditions (2.17) we need to consider $C_n = F_n = S_n = B_n = 0$ for all x.

On substituting the equation (3.1) - (3.4) to the linearized governing equations, we get differential equations:

$$\left(\xi\frac{d^2}{dx^2} - n^2\pi^2\right)D_n + \xi R_a\frac{dG_n}{dx} - \xi R_S\frac{dH_n}{dx} + T_a n\pi A_n = 0, \tag{3.5}$$

$$\chi A_n + T_a n\pi D_n = 0, \tag{3.6}$$

$$P_c\left(\zeta\frac{d^2}{dx^2} - n^2\pi^2\right)H_n - \frac{dD_n}{dx} = \sigma H_n, \tag{3.7}$$

$$\left(\eta\frac{d^2}{dx^2} - n^2\pi^2\right)G_n + p_m\left(\zeta_1\frac{d^2}{dx^2} - n^2\pi^2\right)H_n - \frac{dD_n}{dx} = \sigma G_n. \tag{3.8}$$

And the boundary conditions for D_n, G_n, A_n and H_n as below

$$D_n\left(\frac{1}{2}\right) = D_n\left(-\frac{1}{2}\right) = 0, \qquad A_n\left(\frac{1}{2}\right) = A_n\left(-\frac{1}{2}\right) = 0,$$

$$G_n\left(\frac{1}{2}\right) = G_n\left(-\frac{1}{2}\right) = 0, \qquad H_n\left(\frac{1}{2}\right) = H_n\left(-\frac{1}{2}\right) = 0. \tag{3.9}$$

We can conclude from equation (2.11) - (2.14) and from boundary condition (2.17) that σ to be real.

Thus, to find critical Rayleigh number Ra_c which is a function of (ξ, η, ζ, χ), for the marginal

stability we can substitute $\sigma = 0$ in the equations (3.7) and (3.8). The set of equations (3.5) to (3.8) together with the bc's (3.9) gives Ra as the eigen value, Ra_c is the smallest eigen value. The general solution is of the form

$$D_n(x, R_a) = \left[C_1 \cos px + C_2 \sin px + C_3 \cos qx + C_4 \sin qx\right] \quad , \quad (3.10)$$

$$G_n(x, R_a) = t\left[r\left(C_1 \sin px - C_2 \cos px\right) + C_3 \sin qx - C_4 \cos qx\right] \quad , \quad (3.11)$$

$$H_n(x, R_a) = s\left[r\left(C_1 \sin px - C_2 \cos px\right) + C_3 \sin qx - C_4 \cos qx\right] \quad , \quad (3.12)$$

$$A_n = \frac{-n\pi T_a}{\xi}\left[C_1 \cos px + C_2 \sin px + C_3 \cos qx + C_4 \sin qx\right] \quad . \quad (3.13)$$

Where, C_1, C_2, C_3 and C_4 are arbitrary constants and

$$p_q = \frac{1}{2\sqrt{\xi}}\left\{\left[\sqrt{R_a\left(\frac{p_m}{P_c}-1\right)+n^2\pi^2\left(2+\frac{T_a{}^2}{\xi}\right)-\frac{R_S}{P_c}+2n^2\pi^2\sqrt{1+\frac{T_a{}^2}{\xi}}}\right]\right.$$
$$\left.\pm\left[\sqrt{R_a\left(\frac{p_m}{P_c}-1\right)+n^2\pi^2\left(2+\frac{T_a{}^2}{\xi}\right)-\frac{R_S}{P_c}-2n^2\pi^2\sqrt{1+\frac{T_a{}^2}{\xi}}}\right]\right\} \quad (3.14)$$

$$r = \frac{q\left(\xi p^2 + n^2\pi^2\left(1+\frac{T_a{}^2}{\xi}\right)\right)}{p\left(\xi q^2 + n^2\pi^2\left(1+\frac{T_a{}^2}{\xi}\right)\right)},$$

$$s = \frac{\xi q^2 + n^2\pi^2\left(1+\frac{T_a{}^2}{\xi}\right)}{q\xi\left(R_a P_c\left(1-\frac{p_m}{P_c}\right)\right)},$$

$$t = \left(P_C - pm\right)\frac{\xi q^2 + n^2\pi^2\left(1+\frac{T_a{}^2}{\xi}\right)}{\xi q\left(R_a P_c\left(1-\frac{p_m}{P_C}\right) - R_S\right)}. \quad (3.15)$$

Here, $p \neq q$ is assured by the boundary conditions at $Ra \neq Ra_c$ .from (3.9) boundary condition we get the non-trivial solution of the given problem when

I. $(1-r)\sin\left(\frac{p+q}{2}\right)-(1+r)\sin\left(\frac{p-q}{2}\right)=0$ and

$C_2 = C_4 = 0$ (3.16)

II. $(1-r)\sin\left(\frac{p+q}{2}\right)+(1+r)\sin\left(\frac{p-q}{2}\right)=0$ and

$C_2 = C_4 = 0$. (3.17)

In the case of isotropic medium where $\xi = \eta = \zeta = \chi$, Ra_c can be calculated by solving the equations analytically. Where else in case of anisotropic medium where $\xi \neq \eta = \zeta \neq \chi$, Ra_c found numerically.

The isotropic porous media case: In this case the condition $\xi = \eta = \zeta = \chi$ is fullfilled if $\frac{\kappa_x}{\kappa_z} = \frac{k_x}{k_z}$, i.e. the proportion of the parallel and perpendicular component of thermal diffusivity and the permeability are equal.

The following condition for case I and II are obtained at $r = 1$

$p - q = 2m\pi$, for $m = 1, 2, 3, 4.....$ (3.18)

It gives

$$R_a = \frac{P_C}{p_m - P_C}\left(4\pi^2\xi m^2 + \frac{R_S}{P_c} - n^2\pi^2\left(2+\frac{T_a{}^2}{\xi}\right) + 2n^2\pi^2\sqrt{1+\frac{T_a{}^2}{\xi}}\right) \quad . \quad (3.19)$$

Where $n = 1, 2, 3, 4.....$ and $m = 1, 2, 3, 4.....$

Critical RayEquation (3.19) the critical Rayleigh number, which is the smallest possible value of R_a

$$Ra_c = \frac{P_C}{p_m - P_C}\left(4\pi^2\xi + \frac{R_S}{P_c} - \pi^2\left(2+\frac{T_a{}^2}{\xi}\right) + 2\pi^2\sqrt{1+\frac{T_a{}^2}{\xi}}\right) \quad . \quad (3.20)$$

For an isotropic medium, the smallest eigen value corresponds to $n = 1$ and $m = 1$

$$Ra_c = \frac{P_C}{p_m - P_C}\left(\begin{array}{l} 4\pi^2\left(\frac{h}{a}\right)^2 + \frac{R_S}{P_c} - \pi^2\left(2 + T_a{}^2\left(\frac{a}{h}\right)^2\right) \\ +2\pi^2\sqrt{1 + T_a{}^2\left(\frac{a}{h}\right)^2} \end{array}\right). \quad (3.21)$$

As the limit $\left(\frac{h}{a}\right) \to 0$ and $T_a \to 0$ the channel tends to infinitesimal horizontal porous layer. In such case critical Rayleigh number $Ra_C = 4\pi^2$ it is in line with a well-known conclusion for the permeable layers [25]. The critical value from the equation (3.21) is not same as the conclusion found for a channel with absolutely insulating walls done by [26]. In case $h = a$, i.e we get a square box, equation (3.21) gives $Ra_c = 8\pi^2$ whereas the result corresponding to perfectly insulating lateral walls gives $Ra_c = 4\pi^2$. Since, in this case the heat transfer over the walls. A greater critical value is expected with conducting lateral wall box.

The flow at the onset of neutral convection is the flow for moderately super Critical Rayleigh number. Since the equations (3.16) and (3.17) coincides when $\xi = \eta = \zeta = \chi$, i.e. when $r = 1$,the boundary value problem gives two linearly independent solutions. It can also seen from (2.11) and (2.14) equations.

Let ψ_0, θ_0, S_0 and ν_0 are the solutions at $R_a = Ra_C$, then $\psi_1 = -\xi R_a \theta_0$, $\theta_1 = \psi_0$ and $\nu_1 = \nu_0$ are linearly independent solutions.

The two set of solutions are given by

$$\psi^{(1)} = Q\cos Kx\sin\pi x\sin\pi z;$$
$$\theta^{(1)} = Qs\sin Kx\sin\pi x\sin\pi z \quad ;$$
$$\nu^{(1)} = \frac{-n\pi T_a}{\xi} Q\cos Kx\sin\pi x\cos\pi z \quad ;$$
$$s^{(1)} = -Q\sin Kx\sin\pi x\sin\pi z,$$
$$\psi^{(2)} = \frac{S}{s}\cos Kx\sin\pi x\sin\pi z;$$
$$\theta^{(2)} = S\sin Kx\cos\pi x\sin\pi z, \quad (3.22)$$
$$\nu^{(2)} = -\frac{St}{s}\sin Kx\cos\pi x\cos\pi z;$$
$$s^{(2)} = -\frac{\pi S T_a}{s\xi}\cos Kx\cos\pi x\sin\pi z \quad (3.23)$$

Where, amplitude constants are Q and S. A symmetric flow pattern having 2n cells is given by equation (3.22), where the number of cells n depends on ξ. A symmetric flow arrangement having of $2n \pm 1$ cells is given by (3.23).

Table 1. Values for Ra_c for different values of ξ and η. The principle diagonal coincide with the isotropic case.

ξ/η	0.125	0.25	0.5	1	2
0.125	51463	26181	13419	6954	3662
0.25	101699	51473	26190	13429	6964
0.5	201691	101719	51493	26210	13449
1	400998	201731	101758	51532	26250
2	798652	401077	201810	101837	51611

(i) The Anisotropic case:

This case deals with the condition $\xi \neq \eta = \zeta \neq \chi$ the non - trivial solutions for D_n, A_n, H_n and G_n when the equations (3.16) and (3.17) are fulfilled. Case I gives the solution in the form of

i). $$D_n(x) = \left[\sin px - \frac{\sin\frac{p}{2}}{\sin\frac{q}{2}}\sin qx\right],$$

$$G_n(x) = -s\left[r\cos px - \frac{\sin\frac{p}{2}}{\sin\frac{q}{2}}\cos qx\right],$$

$$H_n(x) = -t\left[r\cos px - \frac{\sin\frac{p}{2}}{\sin\frac{q}{2}}\cos qx\right],$$

$$A_n(x) = \frac{-n\pi T_a}{\chi}\left[\sin px - \frac{\sin\frac{p}{2}}{\sin\frac{q}{2}}\sin qx\right],$$

and for case ii).

$$D_n(x) = \left[\cos px - \frac{\cos\frac{p}{2}}{\cos\frac{q}{2}} \cos qx \right],$$

$$G_n(x) = -s \left[r \sin px - \frac{\cos\frac{p}{2}}{\cos\frac{q}{2}} \sin qx \right],$$

$$H_n(x) = t \left[r \sin px - \frac{\cos\frac{p}{2}}{\cos\frac{q}{2}} \sin qx \right],$$

$$A_n = \frac{-n\pi T_a}{\chi} \left[\cos px - \frac{\cos\frac{p}{2}}{\cos\frac{q}{2}} \cos qx \right].$$

Solutions (i) and (ii) are defined for an large numbers of eigen values. Let two smallest eigen values in each of the above case Ra_1 and Ra_2. These values will exist at $n = 1$. Form equation (3.16) and (3.17) Ra_1 and Ra_2 are calculated for a given value of ξ, η, ζ and χ. Critical Rayleigh number $Ra_c = \{Ra_1 \text{ and } Ra_2\}$ .Normally Ra_1 and Ra_2 are not equal, it means there exist an exclusive values for $Ra_1 \text{ and } Ra_2$ i.e. at the convection there exist a different laminar flow pattern.

IV. SUMMARY

In this study, the effect of uneven temperature gradient on the free convection in a horizontal rectangular box in three dimensions is investigated. The three dimensional problem is transformed to a two dimensional double diffusive convection problem, in which diffusing components are temperature and solute in a anisotropic and isotropic rectangular channels. Channel is considered to heat conducting and impermeable. The channel is heated non- uniformly from below and added solutes to build a linear concentration and temperature distributions in the perpendicular directions. Apart from Boussinesq approximation, which states density remains constant throughout the momentum equation except for the body force and also the following assumptions have been considered.

- Large heating at the walls implies the non-dimensional parameters Darcy-Prandtl numbers are large and hence the inertial and viscous terms are neglected in the momentum equation.
- Flow is symmetric with respect to Y-axis and thereby, introduced the stream function which enables to determine the critical Rayleigh number and solutal Rayleigh number based on the linear stability theory.

The critical Rayleigh number Ra_c obtained by solving the resulting eigen value problem for $(\xi \neq \eta = \zeta \neq \chi)$ in the anisotropy case, whose eigen value is found to be

$$Ra_C = \frac{1}{1-p_m} \left\{ \pi^2 \left[4\eta + \left(1 + \sqrt{\frac{\eta}{\xi}\left(1 + \frac{T_a^{\,2}}{\chi}\right)} \right)^2 \right] + R_s \right\}.$$

The critical Rayleigh number for the corresponding isotropic case $(\xi = \eta = \zeta = \chi)$ as a particular case of the above equation whose eigen value is found to be

$$Ra_c = \frac{P_C}{p_m - 1} \left(4\pi^2 \xi + R_S - \pi^2 \left(2 + \frac{T_a^{\,2}}{\xi} \right) + 2\pi^2 \sqrt{1 + \frac{T_a^{\,2}}{\xi}} \right)$$

The result is in accordance with the previous result, when $T_a = 0$ it reduces to Rayleigh number found in the non-rotating case , when $T_a = 0$ and $\xi = \eta = \zeta = \chi$ (in the isotropic case), as the limit $\frac{h}{a} \to 0$ it reduces to the standard results $Ra_c = R_S + 4\pi^2$ and $Ra_c = 4\pi^2$ when $R_S = 0$ in the absence of the second diffusing components which is in line with the acclaimed result for the porous layers [25]. Two sets of solution which are linearly independent are derived, presents a different nice steady flow patterns at moderately super critical Rayleigh number.

Fig. (8) Represents the plotted graph of critical Rayleigh number versus ratio of permeability to thermal diffusivity. The observation shows that the critical Rayleigh number Rac varies inversely with ratio ξ / η . The critical Rayleigh number are further increases with increasing Taylors number, Solutal Rayleigh number and the effects of rotation therefore, is to destabilize the system more significantly. Observation from Steady flow Patterns.

V. CONCLUSION

Using the similarity transformation we transferred the partial differential equation to ordinary differential equation and Fourier series analysis has been applied to obtained the solution of ordinary differential equations to know the critical Rayleigh numbers, stream function and isotherms of the physical domain to understand the effect of dufour and coriolis force on classic Rayleigh -Bènard problem for an laminar, viscous, unsteady incompressible fluid flow heated from below is extended to 3-dimesional convection in a finite geometry with isotropic and anisotropic porous media rotating with constant angular velocity

The following observations have been main in flow pattern of the streamlines and isothermal lines.

- The number of cells found to be increased with the increase in the Taylor's number for both isotropic and anisotropic cases. Fig. (2) and (4). Increase in Taylor's number increases the coriolis force, which intern increases the number of rotation. Increase in rotation increases the streamlines and isothermal lines.
- The isothermal lines show the increase in the oscillatory flow behaviour with rotation in anisotropic case. Fig. (7)
- The number of cell found to be decreased with increase in aspect ratio and thermal diffusivity in the anisotropic case. Fig. (5) and (6)
- The isotherm becomes more and more flattened with the anisotropy.

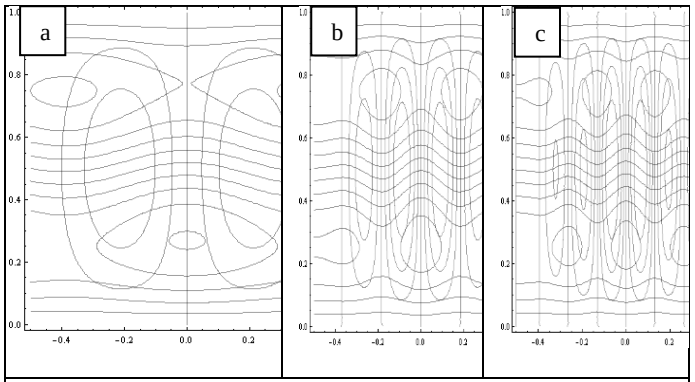

Fig. 2. Flow patternIsothermal lines and Stream lines in isotropic case (T_a-varying)

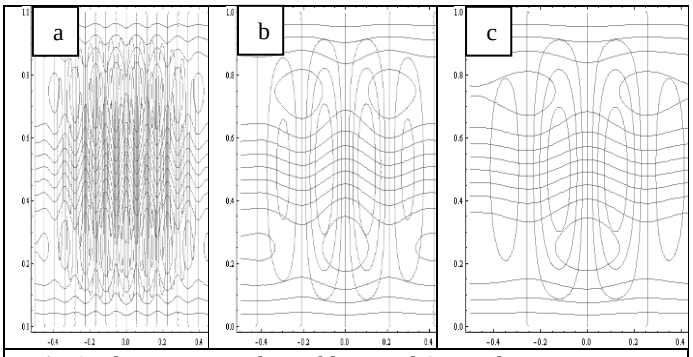

Fig. 3. Flow patternIsothermal lines and Stream lines in isotropic case (ξ-varying)

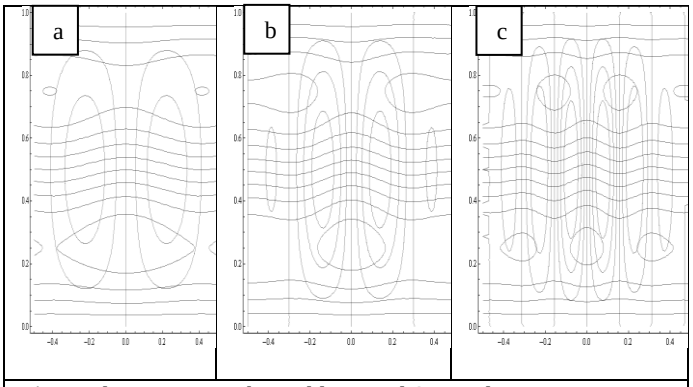

Fig. 4. Flow patternIsothermal lines and Stream lines in anisotropic case (T_a-varying)

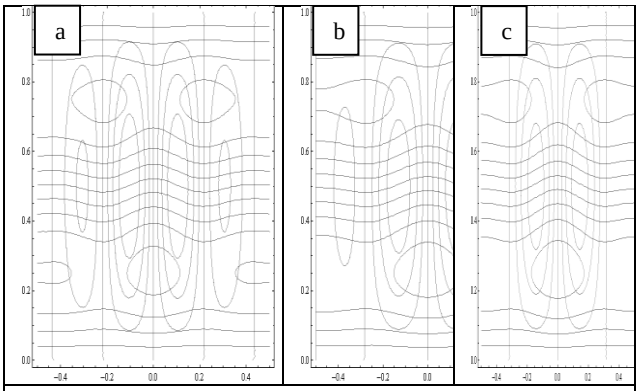

Fig. 6. Flow patternIsothermal lines and Stream lines in anisotropic case (χ-varying)

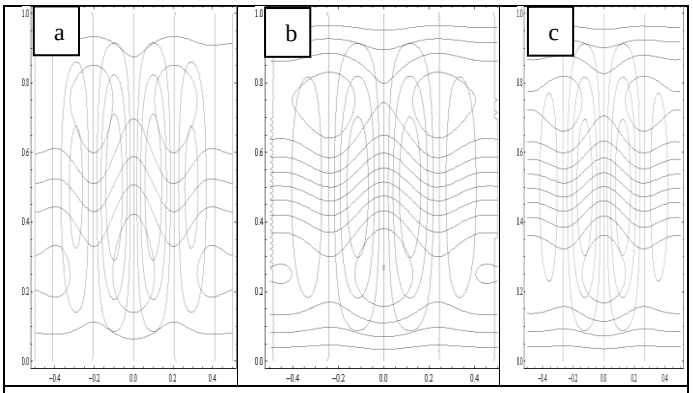

Fig. 7. Flow patternIsothermal lines and Stream lines in anisotropic case (η-varying)

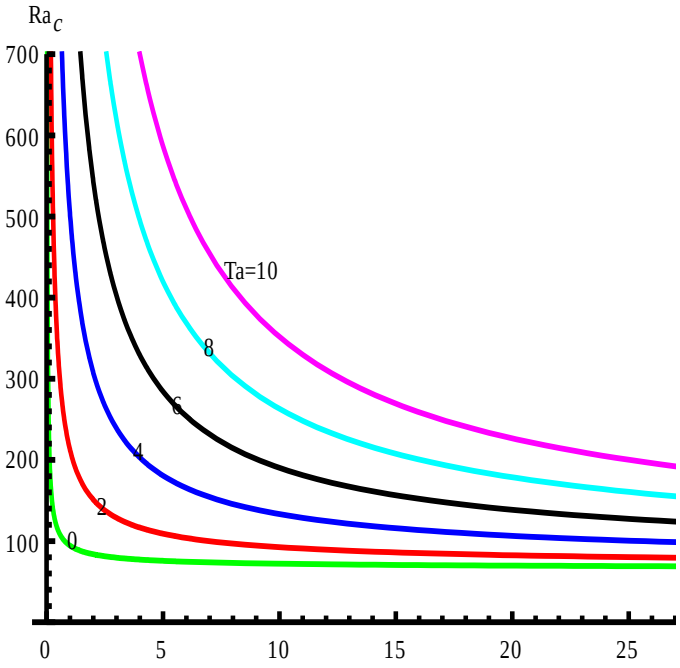

Fig. 8. Plot Ra_c vs ξ / η (Rs=50, ξ=0.5, η=0.125)

Acknowledge

The authors are Thankful to New Horizon College of Engineering,Bangalore, 560103, Ramaiah Institute of Technology, Bangalore-560054, and Cambridge Institute of Technology, Bangalore-560036,. For providing the opportunity to have this collaborative research work. Without their positive support this work would not have been possible.

VI. REFERENCES

[1] Sathish Kumar, M., Sandeep, N., Rushi Kumar, B., & Dinesh, P. A. (2017). A comparative analysis of magnetohydrodynamic non-Newtonian fluids flow over an exponential stretched sheet. Alexandria Engineering Journal.

[2] Suresh Babu, R., Kumar, B. R., & Dinesh, P. A. (2018). Soret and Dufour Effects on MHD Mixed Convection Flow over a Vertical Plate with Variable Fluid Properties. Defect and Diffusion Forum, 389, 1–17.

[3] J. Yan, S.K. Chou, U. Desideri, X. XiaInnovative and sustainable solutions of clean energy technologies and policies (Part II), Appl Energy, 136 (2014), pp. 756-758.

[4] H. Cho, A.D. Smith, P. Mago, Combined cooling, heating and power: a review of performance improvement and optimization Appl Energy, 136 (31) (2014), pp. 168-185. J. Yan, S.K. Chou, U. Desideri,

[5] X. Xia, Innovative and sustainable solutions of clean energy technologies and policies (Part I) Appl Energy, 130 (2014), pp. 447-449..

[6] U. Erturun, K. Erermis, K. Mossi, Influence of leg sizing and spacing on power generation and thermal stresses of thermoelectric devices Applied Energy, 159 (2015), pp. 19-27.doi. 10.1016/j.apenergy.2015.08.112.

[7] Gelfgat, A. Y., Bar-Yoseph, P. Z., & Solan, A. (2001). Effect of axial magnetic field on three-dimensional instability of natural convection in a vertical Bridgman growth configuration. Journal of Crystal Growth, 230(1-2), 63–72.

[8] Yang KT. Transitions and bifurcations in laminar buoyant flows in confined enclosures. J Heat Transfer 1988;110:1191–204.

[9] Koschmieder EL. Be´nard cells and taylor vortices. Cambridge: Cambridge Univ. Press; 1993.

[10] Fusegi T, Hyun JM, Kuwahara K, Farouk B. A numerical study of three dimensional natural convection in a differentially heated cubical enclosure. Int J Heat Mass Transfer 1991;34(6):1543–57.

[11] Janssen RJA, Henkes RAW, Hoogendoorn CJ. Transition to time periodicity of a natural convection flow in a 3D differentially heated cavity. Int J Heat Mass Transfer 1993;36(11):2927–40

[12] G. de Vahl Davis, Natural convection of air in a square cavity: a bench mark numerical solution, International journal for numerical methods in fluids 3 (3) (1983) 249–264.

[13] M. Hortmann, M. Peric´, G. Scheuerer, Finite volume multigrid prediction of laminar natural convection: Bench-mark solutions, Int. J. Numer. Methods Fluids 11 (2) (1990) 189–207.

[14] T. Saitoh, K. Hirose, High-accuracy bench mark solutions to natural convection in a square cavity, Comput. Mech. 4 (6) (1989) 417–427.

[15] P. Le Quéré, Accurate solutions to the square thermally driven cavity at high Rayleigh number, Comput. Fluids 20 (1) (1991) 29–41.

[16] M. Ravi, R. Henkes, C. Hoogendoorn, On the high-Rayleigh-number structure of steady laminar natural-convection flow in a square enclosure, J. Fluid Mech. 262 (1994) 325–351.

[17] G.W.D.C. Wan, BSV Patnaik, A new benchmark quality solution for the buoyancy-driven cavity by discrete singular convolution, Numer. Heat Transf.: Part B: Fundam. 40 (3) (2001) 199–228.

[18] G.D. Mallinson, G.D.V. Davis, Three-dimensional natural convection in a box: a numerical study, J. Fluid Mech. 83 (01) (1977) 1–31.

[19] G. Labrosse, E. Tric, H. Khallouf, M. Betrouni, A direct (pseudo-spectral) solver of the 2D/3D stokes problem: transition to unsteadiness of natural-convection flow in a differentially heated cubical cavity, Numer. Heat Transf. 31 (3) (1997) 261–276.

[20] F. Trias, M. Soria, A. Oliva, C. Pérez-Segarra, Direct numerical simulations of two-and three-dimensional turbulent natural convection flows in a differentially heated cavity of aspect ratio 4, J. Fluid Mech. 586 (2007) 259– 293.

[21] F. Trias, A. Gorobets, M. Soria, A. Oliva, Direct numerical simulation of a differentially heated cavity of aspect ratio 4 with Rayleigh numbers up to 10 11– part I: numerical methods and time-averaged flow, Int. J. Heat Mass Transf. 53 (4) (2010) 665–673.

[22] R. Janssen, R. Henkes, C. Hoogendoorn, Transition to time-periodicity of a natural-convection flow in a 3D differentially heated cavity, Int. J. Heat Mass Transf. 36 (11) (1993) 2927–2940.

[23] E. Tric, G. Labrosse, M. Betrouni, A first incursion into the 3D structure of natural convection of air in a differentially heated cubic cavity, from accurate numerical solutions, Int. J. Heat Mass Transf. 43 (21) (2000) 4043– 4056.

[24] J. Salat, S. Xin, P. Joubert, A. Sergent, F. Penot, P. Le Quere, Experimental and numerical investigation of turbulent natural convection in a large air-filled cavity, Int. J. Heat Fluid Flow 25 (5) (2004) 824–832.

[25] Bories, “Natural Convection in porous media”, Advances in Transport Phenomena in Porous Media, NATO ASI Series book series, Vol. 128, pp 77-141.

[26] Sutton, F. M. (1970). Onset of Convection in a Porous Channel with Net Through Flow. Physics of Fluids, 13(8), 1931.